ELSEVIER

Characterization of chemical properties, unit cell parameters and particle size distribution of three zeolite reference materials: RM 8850 – zeolite Y, RM 8851 – zeolite A and RM 8852 – ammonium ZSM-5 zeolite

S. Turner [a,*], J.R. Sieber [a], T.W. Vetter [a], R. Zeisler [a], A.F. Marlow [a],
M.G. Moreno-Ramirez [a,1], M.E. Davis [b], G.J. Kennedy [c], W.G. Borghard [c],
S. Yang [d,2], A. Navrotsky [d], B.H. Toby [e,3], J.F. Kelly [f], R.A. Fletcher [a],
E.S. Windsor [a], J.R. Verkouteren [a], S.D. Leigh [g]

[a] *Chemical Science and Technology Laboratory, National Institute of Standards and Technology, Gaithersburg, MD 20899, United States*
[b] *Division of Chemistry and Chemical Engineering, California Institute of Technology, Pasadena, CA 91125, United States*
[c] *ExxonMobil Research and Engineering, Annandale, NJ 08801, United States*
[d] *Thermochemistry Facility and NEAT ORU, University of California at Davis, Davis, CA 95616, United States*
[e] *NIST Center for Neutron Research, National Institute of Standards and Technology, Gaithersburg, MD 20899, United States*
[f] *Materials Science and Engineering Laboratory, National Institute of Standards and Technology, Gaithersburg, MD 20899, United States*
[g] *Information Technology Laboratory, National Institute of Standards and Technology, Gaithersburg, MD 20899, United States*

Abstract

Zeolites have important industrial applications including use as catalysts, molecular sieves and ion exchange materials. In this study, three zeolite materials have been characterized by the National Institute of Standards and Technology (NIST) as reference materials (RMs): zeolite Y (RM 8850), zeolite A (RM 8851) and ZSM-5 zeolite (RM 8852). They have been characterized by a variety of chemical and physical measurement methods: X-ray fluorescence (XRF), gravimetry, instrumental neutron activation analysis (INAA), nuclear magnetic resonance (NMR), calorimetry, synchrotron X-ray diffraction, neutron diffraction, laser light extinction, laser light scattering, electric sensing zone, X-ray sedimentation, scanning transmission electron microscopy (STEM), scanning electron microscopy (SEM) and optical microscopy. The chemical homogeneity of the materials has been characterized. Reference values are given for the major components (major elements, loss on ignition [LOI] and loss on fusion [LOF]), trace elements and Si/Al and Na/Al ratios. Information values are given for enthalpies of formation, unit cell parameters, particle size distributions, refractive indices and variation of mass with variation in relative humidity (RH). Comparisons are made to literature unit cell parameters. The RMs are expected to provide a basis for intercomparison studies of these zeolite materials.
© 2007 Elsevier Inc. All rights reserved.

Keywords: Reference materials; Zeolite Y; Zeolite A; ZSM-5; Zeolites

1. Introduction

Microporous aluminosilicate zeolites have widespread industrial application [1]. Traditional uses include: as a catalyst for cracking of high molecular weight hydrocarbons to shorter chain hydrocarbons in the petrochemical industry, for water softening in powder laundry detergents and other ion exchange applications, as drying agents of organic solvents, for waste water treatment and for gas separations [2,3]. More advanced applications for zeolites being investigated include use as chemical sensors, as molecular sieve membranes, for long term toxic waste storage, as nonlinear optical materials and as hosts for semiconductor quantum dots, molecular wires, and lasing dyes [1,4–9]. Considerable basic research has been conducted with the goal of understanding and modifying zeolites for specific applications. For instance, NASA has hosted research into zeolite growth under reduced gravity conditions over the past decade [10]. Recently, organic–inorganic hybrid zeolites have been developed which may lead to a suite of broadened applications [11].

Despite the many current industrial applications of zeolites and the ongoing research into new applications, development of standards for intercomparison of research has been limited. The Federal Institute for Materials Research and Testing of Germany has produced a certified reference material, BAM-P107, in which the specific micropore volume and median pore width of a faujasite type zeolite are certified [12]. Additional information is given for Langmuir specific surface area and density. The material has been accepted as a European Reference Material, ERM-FD107. In general, however, chemical, structural and physical property studies of zeolites are performed on materials synthesized by scientists or on materials obtained from zeolite manufacturers. Neither source is optimum for intercomparison studies over time as the synthesis conditions used by the scientists or manufacturers may produce zeolites with slightly different chemical or physical properties under different conditions. Additionally, the availability of the material might be subject to market conditions experienced by the industry.

A National Science Foundation supported workshop was conducted at the California Institute of Technology in 1995 to discuss the need for reference materials in the zeolite community. A recommendation was made that the National Institute of Standards and Technology (NIST) develop such standards. Materials as produced for industrial applications were donated to NIST. Work was undertaken to develop reference materials for three common zeolites – zeolite Y, zeolite A, and ZSM-5 zeolite. The major components, trace elements and elemental ratios were characterized as reference values; enthalpies of formation, unit cell parameters, particle size distributions, refractive indices and variation of mass with variation in relative humidity (RH) were characterized as information values (reference values are noncertified values that are the best estimate of the true value; information values are noncerti-

fied values that have insufficient information to assess uncertainty [13]). The zeolites are being issued as reference materials: RM 8850 (zeolite Y), RM 8851 (zeolite A), and RM 8852 (ammonium ZSM-5 zeolite) [14–16] and are available from NIST [17]. This work describes the preparation and characterization of these materials.

2. Experimental

2.1. Material preparation

Synthetic zeolite Y, zeolite A and ammonium ZSM-5 zeolite production-type materials were donated by major zeolite manufacturers. The zeolite Y was shipped to NIST in a large drum with a metal lining, the zeolite A in paper bags and the ammonium ZSM-5 in a large drum with a porcelain lining. At NIST, the samples were scooped out of the original containers and placed into aluminized bags using an alternate shovel method. In this procedure, a scoop was taken from the container and placed into a bag, the next scoop taken from the container was placed in another bag, etc. The procedure was repeated until the original container was empty. This procedure was done to ensure that each bag contained samples from all parts of the original container. Each bag contained less than 10 kg of material.

Sample spin riffling and bottling were conducted by NIST to Laboratory Quality Services International (LQSI), a division of Commercial Testing & Engineering Co. (CT&E)[4] under contract to NIST. Each bag of zeolite was spin riffled into bottles that contained 35–40 g of material.

2.2. Chemical analyses

2.2.1. Mass variation with relative humidity variation

Experiments were conducted to: (1) determine the approximate change of mass of the zeolite materials with variation in ambient relative humidity (RH) and (2) test an assumption that the zeolites would reach a stable mass within 48 h at $\approx$50% RH. Protocols in ASTM Standard Practice E 104-02 were followed for maintaining constant RH by means of aqueous solutions [18].

For each zeolite, approximately 1 g of material was placed in an aluminum weighing dish. The samples were placed in a hydrator (sealable glass container) with a saturated salt solution of $MgCl_2 \cdot 6H_2O$ and allowed to equilibrate to the water vapor pressure of the salt solution at 33% $\pm$ 2% RH over several days. The hydrator with the sample was placed in a glove box containing a weighing scale and several pans of $MgCl_2 \cdot 6H_2O$ salt in solution.

After the glove box reached 33% ± 2% RH, the sample was removed from the hydrator, the sample mass determined, and the sample placed back in the hydrator. The pans of $MgCl_2 \cdot 6H_2O$ salt solutions in the glove box were exchanged for pans containing $Mg(NO_3)_2 \cdot 6H_2O$ salt solutions. After the glove box stabilized at approximately 54% ± 2% RH, the sample was removed from the hydrator, placed on the scale in the glove box and its mass monitored at 1-min intervals for approximately the first hour and periodically over the next several days.

2.2.2. Chemical homogeneity, major components and trace elements

Chemical homogeneity was tested for Na, Al, Si, K, Ca, Fe, Zn, and Zr for each zeolite using X-ray fluorescence (XRF) spectrometry. RM 8851 was additionally tested for S. Twenty bottles of each zeolite were selected using a stratified random sampling procedure. Duplicate specimens were prepared from each bottle for a total of 40 specimens. Each specimen was weighed to 3.5 g, formed into a briquette and allowed to equilibrate with the environment in the enclosed sample changer of the X-ray spectrometer, nominally 27.5 °C and 36% relative humidity. Recordings from an Omega thermometer/hygrometer showed the temperature and humidity to be stable within ±1 °C and ±1% RH, respectively. Homogeneity measurements were performed in a helium atmosphere.

Quantitative XRF determinations of Na, Al, Si and Fe were performed for each zeolite by obtaining duplicate samples from each of eight units (or bottles) of zeolite (approximately 750 mg for RM 8850 and RM 8851; approximately 500 mg for RM 8852). The samples were placed into a glove box equilibrated to 54% RH by means of a $Mg(NO_3)_2 \cdot 6H_2O$ slurry. After at least 48 h in the glove box, the samples were weighed on a scale in the glove box at 54% RH and 22 °C. Each weighed sample was transferred to a platinum crucible, combined with $Li_2B_4O_7$ flux, fused at 1100 °C and cast as beads for XRF measurements. Synthetic calibration standards were prepared by borate fusion and used for a matrix-independent calibration [19].

Instrumental neutron activation analyses (INAA) for Na and Al were performed on approximately 100 mg samples from six units of each zeolite. The samples were conditioned for at least 48 h in a glove box containing $Mg(NO_3)_2 \cdot 6H_2O$ in solution. The samples were then weighed on a scale in the glove box (at 53–54% RH and 20–21 °C) and sealed. Elemental standards were prepared by dispensing on filter paper standard solutions of high-purity metals and high-purity NaCl dissolved in high-purity nitric acid and high-purity water. After drying, the residue was pelletized. Control samples were formed from high-purity Al foils and from micropellets of SRM 40 h (sodium oxalate). Irradiation of samples was carried out for 30 s in the RT-4 pneumatic facility of the NIST Center for Neutron Research at a thermal neutron fluence rate of 3.3×10^{13} cm^{-2} s^{-1}. Two gamma-ray counts were carried out with each of the samples, controls and standards.

The first count of the samples was 5 min after 15 min decay; the second count was 30 min after 2 d decay.

Gravimetry analyses for Si were performed on samples from each of eight units of zeolite (for RMs 8850 and 8851 sample mass ≈0.5–0.9 g, for RM 8852 sample mass ≈0.45–0.6 g). The samples were conditioned in a hydrator containing a saturated $Mg(NO_3)_2 \cdot 6H_2O$ solution and were periodically removed from the hydrator over a time span of about 20 d and weighed until a stable mass was attained (temperature ranged from 19 °C to 23 °C). The silicon was determined gravimetrically by a several-step process: (1) fusing the hydrated samples with Na_2CO_3, (2) dissolving the fused melt in water, (3) dehydrating the Si in hydrochloric acid (HCl) over a steam bath to form impure SiO_2, (4) filtering off the impure SiO_2, (5) igniting the impure SiO_2 to constant mass at 1100 °C, (6) volatilizing the SiO_2 with hydrofluoric acid (HF), and (7) igniting the remaining sample to constant mass at 1100 °C. Silicon in the filtrate was determined by graphite furnace atomic absorption spectrometry for RM 8850 and RM 8851 and by XRF for RM 8852.

To determine loss on ignition (LOI) at 1000 °C, samples were taken from each of eight units of each zeolite (for RMs 8850 and 8851, a sample mass of ≈0.5–0.9 g; for RM 8852, a sample mass of ≈0.45–0.6 g) and conditioned in a hydrator containing $Mg(NO_3)_2 \cdot 6H_2O$ in solution. The samples were periodically removed from the hydrator over a time span of about 20 d and weighed until a stable mass was attained. Samples were transferred to a platinum crucible and heated slowly to about 120 °C. After 30 min, the sample was heated to 1000 °C for 2 h and removed to a desiccator containing anhydrous $Mg(ClO_4)_2$. After at least 3 h of cooling to the ambient laboratory temperature, the samples were weighed. Heating to 1000 °C was repeated to check for constant mass.

Loss on fusion (LOF) values were determined upon formation of glass beads for XRF analyses. The LOF values were calculated from a number of experimentally determined parameters: mass of zeolite specimen, mass of flux, loss on ignition of the flux at 1100 °C, and total glass formed during fusion. LOF is comparable but not equivalent to LOI because ignition does not involve a flux and because a measurable amount of LiI is added in the fusion process as a nonwetting agent.

INAA analyses for trace elements were performed by obtaining samples of approximately 5 g from each of eight units of zeolite and conditioning them in a hydrator containing $Mg(NO_3)_2 \cdot 6H_2O$ in solution. The samples were then removed from the hydrator and subsampled into 250 mg portions; two subsamples from each unit were weighed directly into polyethylene irradiation bags and sealed. The subsampling, weighing and sealing were done under ambient laboratory conditions. Elemental standards were prepared by dispensing on filter paper solutions containing known amounts of the elements combined according to nuclear and chemical properties of the elements [20]. After drying, the residue was pelletized. Control samples

were prepared from SRM 2704. Irradiation of samples was carried out in the RT-4 pneumatic facility of the NIST Center for Neutron Research. Irradiation time for RM 8850 and RM 8851 was 4 h + 4 h with a 180° inversion of the irradiation capsule after the first 4 h for flux homogeneity. For RM 8852, irradiation time was 6 h + 6 h with a 180 degree inversion of the irradiation capsule after the first 6 h. Two or three gamma-ray counts were carried out with each of the samples, controls and standards. For RM 8850 and RM 8851, the first count was 1.5 h after 8 d decay; the second count was 8 h after at least 20 d decay. A third count for RM 8851 was 24 h after 200 d decay. For RM 8852, the first count was 1.5 h after 2 d decay, the second count was 12 h after at least 20 d decay.

2.2.3. NMR analyses

Three types of magic angle spinning nuclear magnetic resonance (MAS NMR) spectra were obtained: ^{29}Si MAS NMR to determine Si/Al ratios, ^{27}Al MAS NMR analyses to determine the coordination of Al, and ^{29}Si cross-polarization (CP) MAS NMR for qualitative indication of the presence of Si nuclei in close proximity to hydrogens or trapped hydrocarbons. The experimental conditions and instrumentation used by the two laboratories that conducted the analyses are summarized in Table 1.

2.2.4. Enthalpy of formation

The enthalpy of formation was measured using the experimental procedure described in Navrotsky [21] and Kiseleva et al. [22,23]. The powdered sample was equilibrated to a saturated $Ca(NO_3)_2$ solution, about 50% RH, at room temperature for at least 2 d. Pellets approximately 15 mg in mass and 3 mm in diameter were prepared and weighed in a room at 25 °C ± 0.5 °C and 50% ± 5% RH. Pellets were dropped into molten $2PbO \cdot B_2O_3$ at 700 °C. The calorimeter was operated under a flow of argon, 30–40 mL/min. The measured heat effect is the solution enthalpy plus the heat content of the sample. Four to seven pellets were analyzed from each of three samples from each zeolite.

2.3. Unit cell determination

Synchrotron X-ray diffraction (XRD) was performed on the three zeolite materials. Samples were hydrated over a $Mg(NO_3)_2 \cdot 6H_2O$ solution for a minimum of 48 h. Samples were removed from the hydrator and loaded into 1.5 mm glass capillaries, but were not sealed. The open capillaries were then returned to the hydration chamber for approximately 24 h and allowed to re-equilibrate. Capillaries were then removed from the chamber and quickly sealed. Diffraction data were collected using the X7A beamline at the National Synchrotron Light Source of the Brookhaven National Laboratory. For RM 8850 and RM 8851, a channel-cut Si (1 1 1) monochromator and a Ge (2 2 0) analyzer were used; for RM 8852 a channel-cut Ge (1 1 1) monochromator and a Ge (2 2 0) analyzer were used. A monochromatic beam with wavelength of 0.119966(7) nm, 0.120001(4) nm, 0.119861(3) nm was used respectively for RM 8850, RM 8851 and RM 8852. Wavelengths were calibrated using SRM 640a (Silicon Line Position [XRD]) and a lattice constant of 0.5430825 nm. Data were collected over the range of 4° 2θ to 45° 2θ with a step size of 0.008°. Count times were 0.8 s per point for RM 8850 and RM 8851 and 1 s per point for RM 8852. Synchrotron data intensities and their associated standard uncertainties were corrected for changes in the ring current, as measured using an ion chamber monitor detector. Full-pattern profile fits using the Le Bail technique were used [24]. Refinements were performed using the General Structure Analysis System (GSAS) package [25].

Neutron diffraction analyses were performed on RM 8850 and RM 8851. Samples were dehydrated by increasing the temperature from ambient to 200 °C over a 12 h time period. The samples were held at 200 °C for 24 h and cooled. After dehydration, the samples were sealed under vacuum and were transferred to a He-filled glovebox where

Table 1a
^{29}Si MAS NMR for Si/Al ratio

	Lab 1	Lab 2
Instrument	Bruker AM-300 NMR	Bruker AMX-200 NMR
Magnetic field strength	59.3 MHz	39.76 MHz
Pulse width ($\pi/2$)	6.5 μs	6 μs
Recycle delay	60 s	60 s
Number of scans	1200–1500	280–720
Line broadening	None	30 Hz

Table 1b
^{27}Al MAS NMR for Al coordination

	Lab 1	Lab 2
Instrument	Bruker AM-300 NMR	Bruker AMX-360 NMR
Magnetic field strength	78.24 MHz	93.84 MHz
Pulse width ($\pi/2$)	22.8 μs	7.5 μs
Excitation pulse width	3.8 μs	1.2 μs
Recycle delay	0.1 s	0.1 s
Number of scans[a]	2000, 80,000	8000
Line broadening	None	50 Hz

[a] For RMs 8850 and 8851, 2000 scans were used; for RM 8852 80,000 scans were used to obtain similar noise levels (Lab 1).

Table 1c
^{29}Si CP-MAS NMR

	Lab 1	Lab 2
Instrument	Bruker AM-300 NMR	Bruker AMX-200 NMR
Magnetic field strength	59.3 MHz	39.76 MHz
Pulse width ($\pi/2$)	6.5 μs	6 μs
Recycle delay	1.5 s	1.5 s
Number of scans	16,000–18,000	38,000–68,000
Line broadening	None	100 Hz

the nominal H_2O level was monitored to be < 5 ppm. Samples were loaded into 12.4 mm internal diameter vanadium containers to a height of approximately 25 mm and sealed with indium wire gaskets. Sample masses were typically 1–1.2 g. Neutron powder diffraction data were collected using the BT-1 32 neutron powder diffractometer at the NIST Center for Neutron Research [26]. A Ge (311) monochromator with a 75° take-off angle, wavelength 0.20783(2) nm, and in-pile collimation of 15 min of arc were used. Data were collected over the range of 1.3° 2θ to 166.3° 2θ with a step size of 0.05° with counting times of approximately 1.8 min per point so that the total scan time was approximately 6 h per sample. Structural refinements were performed using the Rietveld technique, using GSAS software [25].

2.4. Particle size analyses

Particle size analyses were performed using laser light scattering, laser light extinction, electric sensing zone, scanning transmission electron microscopy (STEM) and scanning electron microscopy (SEM). To obtain representative samples for the analyses, a series of sample size reduction steps were done to randomly chosen units of material using a spin riffling apparatus. Bottles of zeolite were split into 16 subsamples using a rotary splitter. One of the 16 subsamples was then randomly selected and further split into eight subsamples using a small rotary spin riffler. An overall riffle split mass reduction of 128 yielded samples of approximately 0.2 g, which is the subsample size used for particle analysis.

Laser light scattering measurements were performed on the three zeolite materials. Two 0.2 g subsamples were selected from each of eight bottles from each zeolite material. Electric mobility measurements were made to aid in selection of an appropriate pH of an aqueous suspension in which the particles would not aggregate due to electrostatic forces. Each 0.2 g subsample was added to 30 mL of filtered, deionized water with pH adjusted to 9.5 for RM 8850 and RM 8851 and to 5 for RM 8852. An ultrasonic horn unit was used to disperse particles in the suspension at a 50 W power level for 4 min for RM 8850 and RM 8851 and 3 min for RM 8852. A Beckman Coulter LS 230 light scattering system was used to make the particle size measurements.

Mie optical models were used to derive the particle size distribution from the laser light scattering data. For such modeling, determination of the refractive indices of the material is necessary. Refractive index measurements made to two decimal places are considered sufficient for this purpose. Refractive index determinations were made on a Leitz Wetzlar optical microscope using refractive index oils from Cargille Laboratories Inc. The ambient temperature was monitored and a temperature correction made to the value for the matching oil. The small particle size of the materials prevented analysis of individual particles so Becke line measurements were made on clumps on materials.

Electric sensing zone measurements were performed on RM 8850 and RM 8851. A subsample from one unit of each zeolite was suspended in water and sonicated for 12 min. The Beckman Coulter Multisizer 3 Coulter Counter instrument used for these measurements was calibrated using SRM 1692 (2.98 μm latex spheres). For a given aperture of diameter D, the working range is from $0.02D$ to $0.60D$. For this material, a 30 μm aperture was used to enable measurements over the range from 0.6 μm to 36 μm. The conductive fluid was an aqueous solution of 4.0% mass fraction NaCl.

Laser light extinction measurements were performed on the three zeolites. A 0.2 g subsample from each of three bottles of the zeolite was randomly chosen. An individual sample was added to 25 mL of filtered, distilled water and the original vial was washed three times with 2 mL aliquots of filtered, distilled water to ensure complete transfer of the zeolites. The suspension was sonicated using a Branson Cell Disruptor 200 operating at approximately 40 W of power for 20 min. After ultrasonifying, a 2 mL aliquot was transferred from the vial into 400 mL of particle-free water. The suspension was homogenized again using the following three-step procedure: (1) shaking for 5 min using a paint mixer, (2) ultrasonifying for 5 min using a Branson 2200 ultrasonic bath and (3) shaking for an additional 15 min on the paint mixer. This suspension was further diluted by transferring a 2 mL aliquot to 400 mL of water. The suspension was then homogenized using the three-step procedure described above. A HIAC/ROYCO (HR-LD 150) system was used for particle size analysis. The response of the HR-LD 150 was calibrated to NIST traceable polystyrene spheres suspended in particle-free water. A blank analysis was run prior to each sample.

X-ray sedimentation measurements were obtained from all materials. The gravitational liquid sedimentation method was used. The suspension was prepared using 0.2 g of sample in 50 mL filtered water. The suspension was sonicated at 50 W power level for 4 min. The practical upper limit on particle size is about 60 μm (determined by laminar flow criteria) and the lower limit is about 0.5 μm (determined by Brownian motion). The zeolite density used for calculations is 1.92 g cm^{-3}.

STEM images were obtained for the three zeolite materials. Samples were prepared by dipping a carbon film grid into the zeolite powder. The grid was examined using a field emission gun FEI CM300 TEM operated in dark field STEM mode. The particles were not sonicated prior to STEM and so the images may not represent the state of dispersion achieved for the optical or electrical instrument analyses that were performed on deagglomerated samples.

SEM images were obtained for RM 8850. Samples were prepared by suspending the zeolite Y zeolite in water and sonicating in an ultrasonic bath for 2 min. The suspension was then shaken in a paint shaker for 15 min. The suspension of zeolite Y powder was filtered onto a polycarbonate filter and the filter was then carbon coated. The sample was examined using a field emission gun Hitachi S-4500 SEM. Only limited attempts were made to disperse the particles and the images may not represent the state of dispersion

achieved for the optical or electrical instrument analyses performed on deagglomerated samples.

2.5. Statistical analysis

Uncertainties in reported mass fraction values were assessed by the CIPM (International Committee for Weights and Measures) approach [27]. For element mass fractions determined from two analytical methods (Na, Al, Si [relative to hydrated mass], and Fe), expanded uncertainties are determined, with coverage factor $k = 2$ (95% confidence), by combining a between-method variance [28] with a pooled, within-method variance, following International Standards Organization (ISO) and NIST guidelines [27,29]. For mass fractions obtained by one analytical method (Si [relative to ignited mass], LOI, LOF, and trace elements except for Fe), the expanded uncertainty, U, is calculated as $U = ku_c$ where u_c is the combined standard uncertainty calculated according to the ISO and NIST Guides [27,29]. The coverage factor, k, is determined from the Student's t-distribution corresponding to the appropriate associated degrees of freedom to achieve 95% confidence for each analyte.

The determination of uncertainties for other reported values are discussed in the footnotes of associated tables.

3. Results

3.1. Chemical analyses

3.1.1. Mass variation with RH variation

Example plots of the change of mass within approximately 1 h or less with change in RH from $33\% \pm 2\%$ to $54\% \pm 2\%$ are shown in Fig. 1. Over 48 h, the experiments showed an increase in mass of approximately 0.55%, 0.4% and 1.25% for RM 8850, RM 8851, and RM 8852, respectively. RM 8851 and RM 8852 remained stable in mass after 48 h in constant humidity; RM 8850 showed a slight gain in mass ($< 0.1\%$) after several additional days of exposure. Given the initial change in mass with short term exposure to a different humidity, weighing of samples in a controlled environment of $54\% \pm 2\%$ RH with no exposure to ambient laboratory humidity is considered the optimum procedure for chemical and structural analysis. The values for mass variation with RH variation are for information only as the uncertainties associated with the values were not determined.

3.1.2. Chemical homogeneity, major components and trace elements

The results of chemical homogeneity testing by XRF showed no statistically significant differences among bottles for Na, Al, Si, Ca, and Fe for the three zeolites and for S for RM 8851. Additionally, there were no statistically significant differences for K, Zn and Zr aside from the RMs indicated in Table 2. A statistical F-test (5% significance) applied to the data for K for RM 8850, Zn for RM 8851
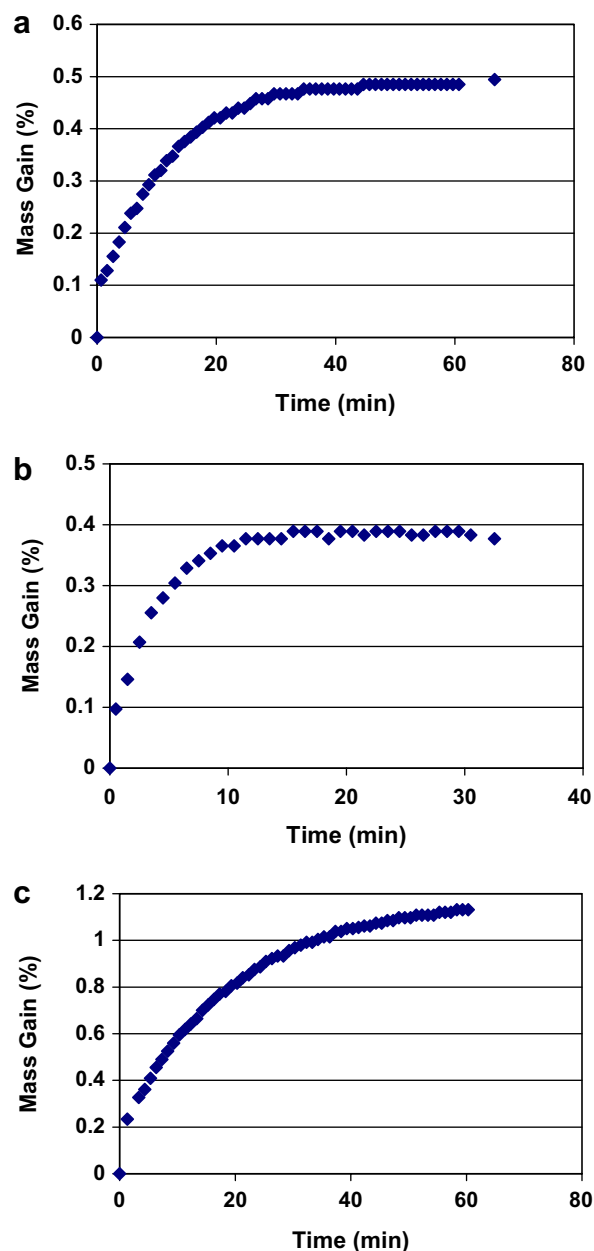

Fig. 1. Example plots of change in mass within approximately 1 h or less of (a) RM 8850, (b) RM 8851, and (c) RM 8852 as ambient humidity was changed from $33\% \pm 2\%$ RH to $54\% \pm 2\%$ RH.

Table 2
Elements inhomogeneously distributed in RMs 8850, 8851, 8852

RM	Element	Mass analyzed (g)[a]	r.s.d. (%)[b]
8850	K	0.03	0.8
8851	Zn	0.5	0.3
8852	Zn	0.5	0.6
8852	Zr	1.0	0.8

[a] Mass of zeolite material viewed by the XRF spectrometer.
[b] Relative standard deviation.

and RM 8852 and Zr for RM 8852 indicates heterogeneity between bottles at the level of precision of the test data.

Relative standard deviations for the elements and the mass analyzed are given in Table 2. For the major elements (Na, Al and Si for RMs 8850 and 8851; Al and Si for RM 8852) specimens as small as 10 mg of material will be representative of the bulk material. For trace element measurements, it is recommended that at least 0.05 g be sampled for RM 8850, 0.5 g for RM 8851 and 1.0 g for RM 8852.

The reference values for the major components of the three zeolites along with methods used in analysis are given in Table 3. For RM 8852, Na is not reported because no Na was detected above the XRF method limit of detection of 0.004% and Na was not analyzed by INAA. Two values are given for silicon for the three materials – one relative to the sample mass equilibrated to ≈54% RH and the second relative to the sample mass ignited at 1000 °C. The Si value relative to the ignited mass should be independent of initial ambient RH and hydration conditions.

The elemental ratios for the three zeolites are given in Table 4. The reference values for Si/Al for all three materials and Na/Al for RMs 8850 and 8851 were calculated from the elemental values reported in Table 3 and the atomic mass of the elements. The Na/Al values for RM 8850 and RM 8851 are approximately one as expected by charge balance considerations. The Na/Al for RM 8851 is 1.0120 ± 0.0074 and the Si/Al ratio is also ≈1.

Reference values for detectable trace elements derived by INAA measurements are given in Table 5. A correction factor was applied to data collected to account for exposure to ambient humidity. Trace element analyses were conducted for Ag, As, Cd, Ce, Co, Cr, Cs, Eu, Fe, Hf, La, Mo, Rb, Sb, Sc, Se, Sm, Sn, Th, W, and Zn. For the three zeolites, concentrations for Ag, As, Cd, Mo, Se, and Sn were at or below the detection limit for the method. Dashes in the table indicate concentrations at or below the

detection limit for the method. Inhomogeneous distributions for Co, Cr, and Cs were noted for RM 8850 and for Co for RM 8851.

3.1.3. NMR analyses

Three types of spectra: ^{29}Si MAS NMR, ^{27}Al MAS NMR and ^{29}Si CP-MAS NMR obtained for the three materials are shown in Figs. 2–4. The ^{27}Al MAS NMR spectra show a single Lorentzian peak for each material corresponding to tetrahedral or framework aluminum.

Table 5
Reference values for detectable trace elements

Element	RM 8850 mass fraction (mg/kg)[a]	RM 8851 mass fraction (mg/kg)[a]	RM 8852 mass fraction (mg/kg)[a]
Ce	2.836 ± 0.066	1.069 ± 0.039	1.708 ± 0.051
Co[b,c]	0.1308 ± 0.0040	0.0646 ± 0.0028	0.1848 ± 0.0051
Cr[c]	1.212 ± 0.053	0.513 ± 0.033	4.48 ± 0.13
Cs[c]	0.0298 ± 0.0031	0.00560 ± 0.00052	–
Eu	0.0345 ± 0.0009	0.02487 ± 0.00078	–
Fe	174.3 ± 2.0	90.8 ± 5.2	222.6 ± 9.4
Hf	0.816 ± 0.019	0.803 ± 0.025	1.337 ± 0.045
La	1.666 ± 0.048	0.534 ± 0.026	0.471 ± 0.014
Rb	0.335 ± 0.042	–	–
Sb	–	–	1.581 ± 0.045
Sc	0.1350 ± 0.0037	0.0591 ± 0.0019	0.0943 ± 0.0030
Sm	0.1861 ± 0.0068	0.1028 ± 0.0061	0.0815 ± 0.0025
Th	0.3601 ± 0.0086	0.1413 ± 0.0046	0.3350 ± 0.0098
W	–	–	2.240 ± 0.068
Zn	19.45 ± 0.99	18.73 ± 0.98	0.749 ± 0.048

[a] See text (Section 2.5) for discussion of uncertainty determinations.
[b] Results from one of 16 analyses for Co was excluded for RM 8851 (sample had a nugget containing high Co and measurable Ag [31 µg/kg ± 1 µg/kg]).
[c] These elements were inhomogeneously distributed for RM 8850.

Table 3
Reference values for major components of RMs 8850, 8851, 8852

Component	RM 8850 mass fraction (%)[a]	RM 8851 mass fraction (%)[a]	RM 8852 mass fraction (%)[a]	Method
Na[b]	7.225 ± 0.094	12.732 ± 0.066	–	XRF, INAA
Al[b]	8.49 ± 0.11	14.766 ± 0.076	1.396 ± 0.015	XRF, INAA
Si[b]	22.52 ± 0.16	15.27 ± 0.10	41.18 ± 0.34	XRF, Grav.
Si[c]	30.336 ± 0.054	19.541 ± 0.045	45.19 ± 0.13	Grav.
LOI[b,d]	25.679 ± 0.095	21.464 ± 0.085	8.50 ± 0.09	Grav.
LOF[b,e]	25.37 ± 0.67	22.1 ± 1.7	8.47 ± 0.38	Grav.

[a] See text (Section 2.5) for discussion of uncertainty determinations.
[b] Value relative to the hydrated sample mass.
[c] Value relative to sample mass ignited at 1000 °C.
[d] Ignited at 1000 °C.
[e] Value relative to sample mass fused at 1100 °C.

Table 4
Reference values for Si/Al and Na/Al ratios determined from element mass fractions[a]

Element ratio	RM 8850 ratio value	RM 8851 ratio value	RM 8852 ratio value	Contributing methods
Si/Al	2.548 ± 0.037	0.9935 ± 0.0082	28.34 ± 0.39	XRF, INAA, Grav.
Na/Al	0.999 ± 0.018	1.0120 ± 0.0074	–	XRF, INAA

[a] The reference ratio values for Si/Al and Na/Al (determined from element mass fractions) are calculated using the reference values of Table 3 and the atomic mass of the elements. The corresponding uncertainties are determined by propagation-of-error [30] for ratios from the unexpanded uncertainties of Table 3, and then expanded by a coverage factor $k = 2$ (95% confidence).
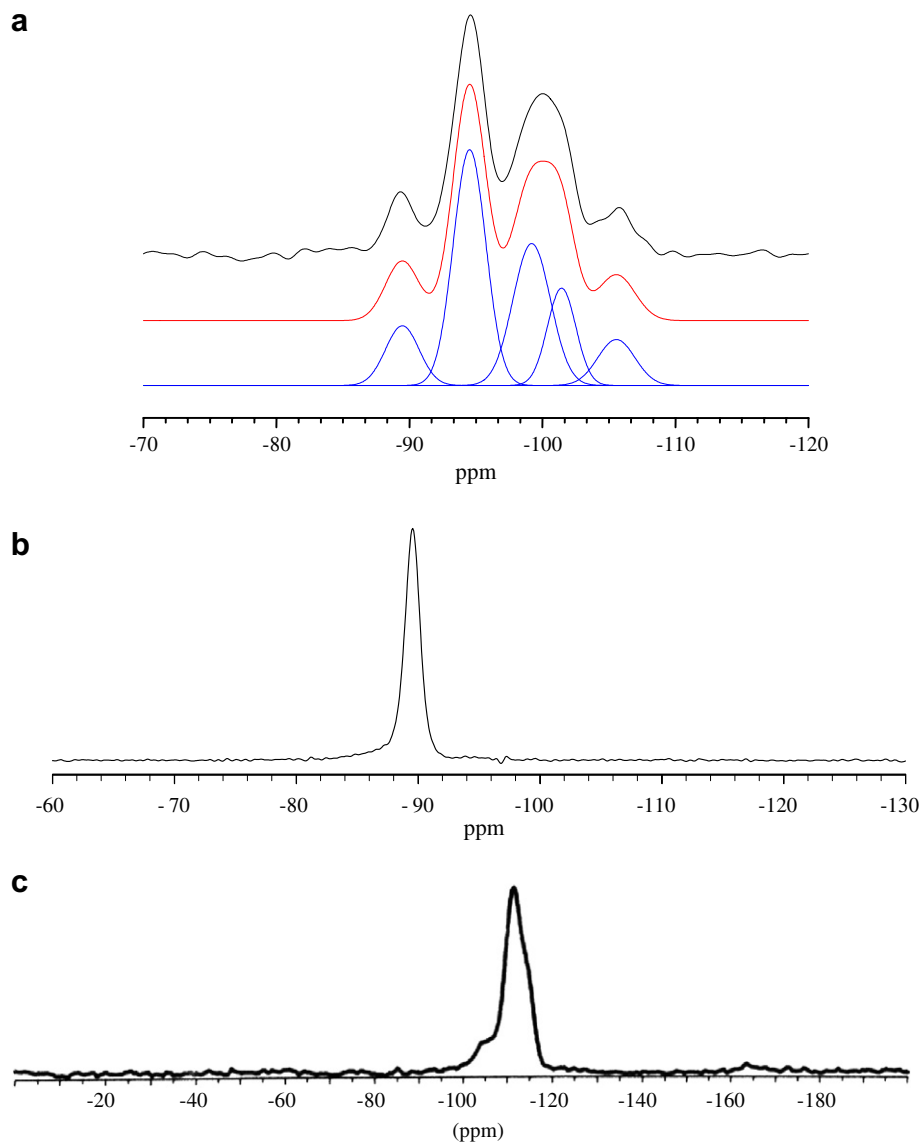
Fig. 2. ^{29}Si MAS NMR spectra obtained from (a) RM 8850, (b) RM 8851, and (c) RM 8852. Figure (a) contains a ^{29}Si MAS NMR spectrum (upper), simulated spectrum (middle) and fitted Gaussian peaks (lower).

There is no evidence for octahedrally coordinated aluminum in the samples.

Information values for the Si to Al ratio determined from ^{29}Si MAS NMR analyses for RM 8850 and RM 8851 are shown in Table 6. The value for RM 8850 is modeled from fitting peaks to the spectra and the value is close to the ratio derived from the elemental analyses given in Table 3. The value for RM 8851 is simply estimated from the single peak observed in the NMR spectra. No value is reported for RM 8852, as the ratios derived from a high Si to Al ratio (>10) are not reliable [31].

3.1.4. Enthalpy of formation

Information values for the enthalpy of formation from constituent oxides and liquid water and constituent elements at 25 °C are given in Table 7. The formation enthalpy of RM 8850 from constituent oxides is −46.74 kJ/mol ± 0.81 kJ/mol, which is in good agreement with that of a similar zeolite, NaY (CBV-100, Aldrich) −42.39 kJ/mol ± 0.86 kJ/mol [32,33]. The formation enthalpy of zeolite A (RM 8851) from constituent oxides, −74.24 kJ/mol ± 0.65 kJ/mol, has not previously been reported. The formation enthalpy of RM 8852 (ZSM-5, a high silica zeolite) is −6.26 kJ/mol ± 0.54 kJ/mol which is in good agreement with that of pure silica MFI zeolite, −6.8 kJ/mol ± 0.8 kJ/mol [34].

3.2. Unit cell determination

The unit cell parameters derived from synchrotron X-ray diffraction measurements of hydrated zeolites are shown in Table 8.

For hydrated RM 8850, measurements were performed using 15 different specimens taken from 12 bottles of
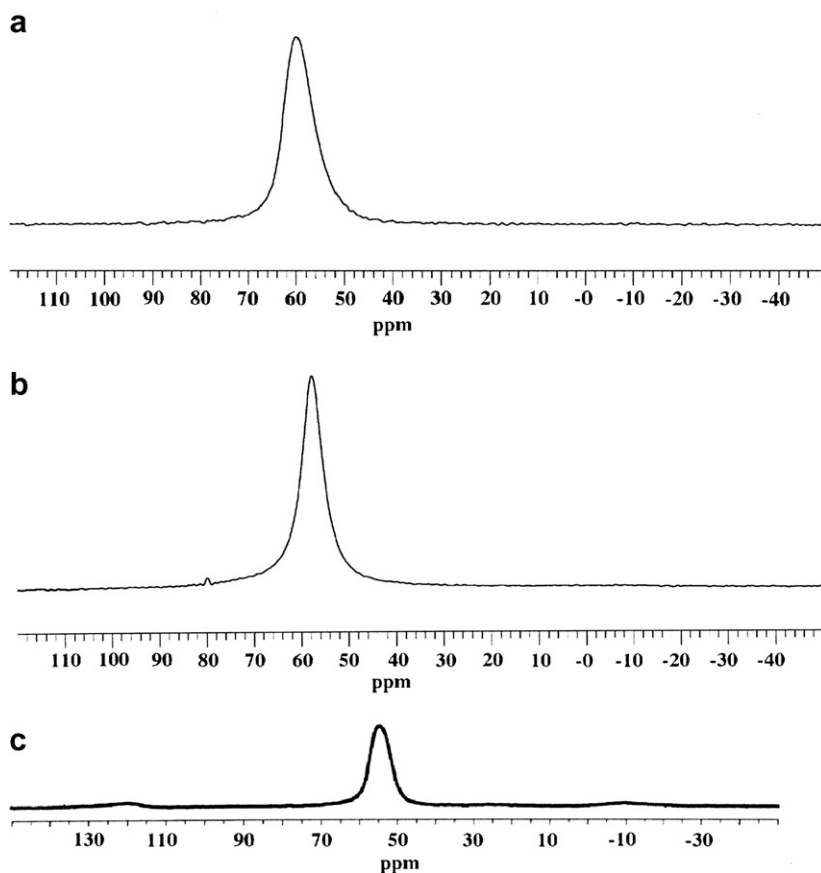
Fig. 3. ^{27}Al MAS NMR spectra obtained from (a) RM 8850, (b) RM 8851, and (c) RM 8852.

zeolite. The result for one sample was rejected as an outlier after a poor seal was noted and the results in Table 8 are an average of 14 specimens. Weighted profile R-factors (R_{wp}) varied over a small range, 0.097 to 0.116, and the overall χ^2 is 1.7, indicating good agreement. The standard uncertainty for an individual measurement is approximately an order of magnitude smaller than the observed standard deviation for the mean unit cell parameter. The data from the collected samples show a slight trend with the samples analyzed later in time showing larger cell parameters. It is not known if this trend and the relatively large overall standard deviation reflect chemical or hydration differences in the specimens or experimental effects. Peaks from an impurity phase were noted, where the strongest impurity peak was ≈0.5% of the strongest zeolite Y peak. The identity of the impurity phase is unknown. The amount of the impurity was not quantified but is presumed small.

For hydrated RM 8851, measurements were performed using 16 different specimens taken from 12 different bottles of zeolite. The results for three samples were determined to be outliers and were discarded. The results in Table 8 are an average of 13 specimens. Weighted profile R-factors (R_{wp}) varied over a small range, 0.110 to 0.146, and overall χ^2 is 1.5, indicating good agreement was obtained. Peaks from an impurity phase were noted where the strongest

impurity peak was ≈1% of the strongest zeolite A peak. This impurity phase was assigned as sodalite and included in the Le Bail fit [24] using a cubic unit cell in space group P-43n with dimensions $a = 0.9976$ nm. The amount of this impurity was not quantified by XRD but is presumed small.

For hydrated RM 8852, measurements were performed using 16 different specimens taken from 12 different samples. The data were fit to an orthorhombic unit cell. Weighted profile R-factors (R_{wp}) varied over a small range, 0.070 to 0.092 and χ^2 ranged from 1.8 to 2.2, indicating good agreement was obtained. The standard deviations of the mean cell parameters listed in Table 8 are significantly larger than the uncertainty for a single measurement. The cell parameters for the individual refinements show a possible trimodal distribution. The source of the differences is assigned to either variation in the sample hydration or composition. No impurity peaks were noted.

The unit cell parameters derived from neutron diffraction measurements of dehydrated zeolites are shown in Table 9. For dehydrated RM 8850, 12 specimens were prepared from 12 samples. The atomic parameters used for refinement of the collected data are shown in Table 10. The results for one sample were rejected as an outlier and the results in Table 9 are an average of 11 specimens. Weighted profile R-factors (R_{wp}) varied over a small range,
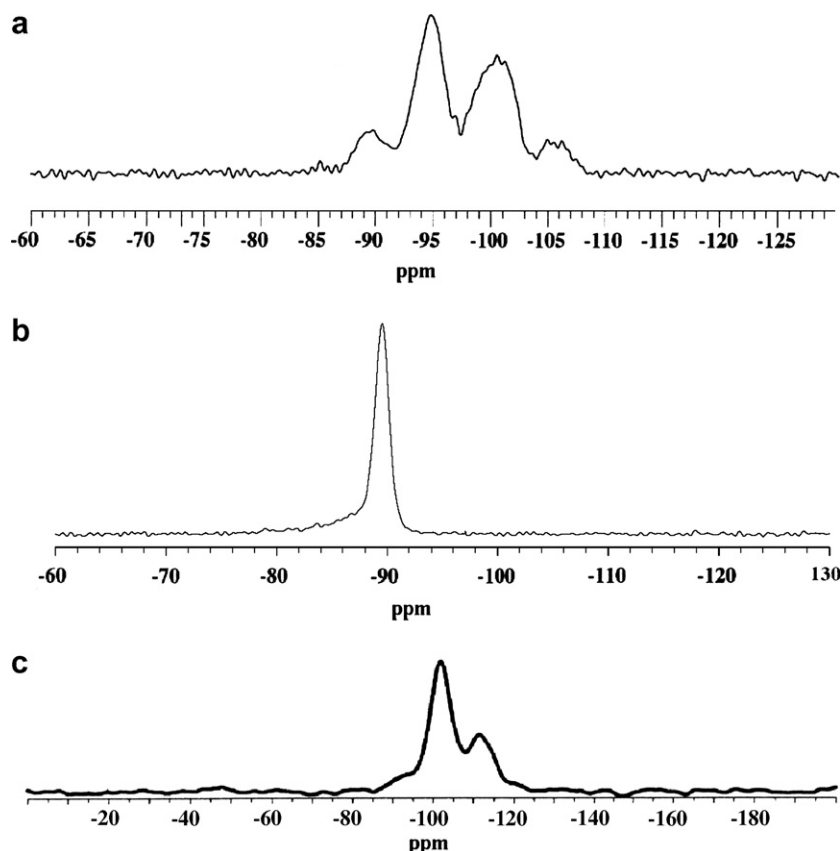
Fig. 4. ^{29}Si CP-MAS NMR spectra obtained from (a) RM 8850, (b) RM 8851, and (c) RM 8852.

Table 6
Information values for Si/Al ratios determined from ^{29}Si MAS NMR analyses

Material	Ratio[a]
RM 8850	2.60 ± 0.06
RM 8851	1
RM 8852	–

[a] The uncertainty value for Si/Al for RM 8850 is an expanded uncertainty about the mean (coverage factor $k = 2$, 95% confidence).

Table 7
Information values for enthalpy of formation from constituent oxides and liquid water, and constituent elements at 25 °C

Constituents	RM 8850 enthalpy of formation (kJ/mol)[a]	RM 8851 enthalpy of formation (kJ/mol)[a]	RM 8852 enthalpy of formation (kJ/mol)[a]
Oxides and liquid water	−46.74 ± 0.81	−74.24 ± 0.65	−6.26 ± 0.54
Elements	−1360.1 ± 1.1	−1365.4 ± 0.9	−990.8 ± 1.1

[a] The uncertainties are propagated from calorimetric data and from literature values for the constituent oxides or elements (coverage factor $k = 2$, 95% confidence).

Table 8
Information values for unit cell parameters of hydrated zeolites

Material	Axis	Unit cell parameter (nm)[a]	Space group
RM 8850	a	2.4697 ± 0.0002	Fd-3m
RM 8851	a	2.4589 ± 0.0002	Fd-3c
RM 8852	a	2.0116 ± 0.0008	Pnma
	b	1.9931 ± 0.0014	
	c	1.3418 ± 0.0009	

[a] The uncertainty is one standard deviation based on 14 samples for RM 8850, 13 samples for RM 8851 and 16 samples for RM 8852.

Table 9
Information values for unit cell parameters of dehydrated zeolites RM 8850 and RM 8851

Material	Axis	Unit cell parameter (nm)[a]	Space group
RM 8850	a	2.4791 ± 0.0003	Fd-3m
RM 8851	a	2.4560 ± 0.0006	Fd-3c

[a] The uncertainty is one standard deviation based on 11 samples for RM 8850 and 11 samples for RM 8851.

data. Similar decompositions of trace impurities have been noted for other zeolites.

For dehydrated RM 8851, 11 specimens were prepared from 11 samples. The atomic parameters used for refinement of the collected data are shown in Table 11. Weighted profile R-factors (R_{wp}) varied over a small range, 0.057 to

0.063 to 0.068, and the overall χ^2 is 1.24. Peaks from the unknown impurity could not be detected in the collected

Table 10
Parameters used for Rietveld refinement of dehydrated RM 8850[a,b]

Atom	x/a	y/a	z/a	Fractional occupancy	$100 \times U_{iso}$	Site multiplicity
T	0.12552 (21)	0.94545 (20)	0.03582 (25)	1	1.38 (10)	192
O1	0.17614 (19)	0.17614 (19)	0.96703 (25)	1	3.5 (2)	96
O2	0.17728 (20)	0.17728 (20)	0.31790 (25)	1	2.5 (2)	96
O3	0.25204 (17)	0.25204 (17)	0.14209 (23)	1	2.5 (2)	96
O4	0.10658 (15)	−0.10658 (15)	0	1	1.4 (2)	96
Na1	0.0550 (5)	0.0550 (5)	0.0550 (5)	0.637 (33)	2.8 (9)	32
Na2	0	0	0	0.41 (5)	5.6 (24)	16
Na3	0.2346 (4)	0.2346 (4)	0.2346 (4)	1	3.0 (4)	32

[a] Column headings correspond to atoms and their fractional coordinates, site occupancy, isotropic thermal parameters (U_{iso}) and site multiplicity.
[b] Values in parentheses represent standard uncertainties in the associated value, where the uncertainty is applied to the final digit(s) of the value. Standard uncertainty is a crystallographic statistic derived from experimental counting statistics propagated via the least-squares covariance matrix [35].

Table 11
Parameters used for Rietveld refinement of dehydrated RM 8851[a,b]

Atom	x/a	y/a	z/a	Fractional occupancy	$100 \times U_{iso}$	Site multiplicity
Si	0	0.09410 (27)	0.18391 (26)	1	1.46 (5)	96
Al	0	0.18751 (34)	0.08929 (34)	1	1.46 (5)	96
O1	0	0.11334 (8)	0.24791 (28)	1	2.46 (3)	96
O2	0	0.14394 (22)	0.14635 (23)	1	2.46 (3)	96
O3	0.05460 (13)	0.05785 (12)	0.17248 (6)	1	2.46 (3)	192
Na1	0.09979 (9)	0.09979 (9)	0.09979 (9)	0.928 (11)	2.11 (16)	64
Na2	0	0.2326 (5)	0.2031 (6)	0.248 (5)	2.11 (16)	96

[a] Column headings correspond to atoms and their fractional coordinates, site occupancy, isotropic thermal parameters (U_{iso}) and site multiplicity.
[b] Values in parentheses represent standard uncertainties in the associated value, where the uncertainty is applied to the final digit(s) of the value. Standard uncertainty is a crystallographic statistic derived from experimental counting statistics propagated via the least-squares covariance matrix [35].

Table 12
Information values for refractive indices

Material	Refractive index	Refractive index value used for Mie modeling
RM 8850	1.442–1.444	1.44
RM 8851	1.446	1.45
RM 8852	1.472–1.474	1.47

0.067, and overall χ^2 is 1.07. Peaks from the sodalite impurity could not be detected in the patterns. Based on pattern simulations, peaks due to a 1–2% sodalite impurity (by mass) would be difficult to detect in the data, setting an upper limit for the impurity level (see further discussion in Section 4.2).

The unit cell values and standard deviations given in Tables 8 and 9 represent multiple measurements. The uncertainty derived for a single measurement is less than the reported standard deviation by a factor of 2–10. The source of the increased variation is not known. Possible causes include chemical variation or variation in water content. The size of the sample used for synchrotron work (<0.02 g), might be small enough to show variation in chemistry that could affect the unit cell dimensions. Additionally, the synchrotron samples were briefly exposed to ambient laboratory humidity prior to sealing. The size of neutron diffraction samples (1–1.2 g), would have been expected to provide homogeneous sampling of the material as it meets the sampling requirements of 0.05 g and 0.5 g for RM 8850 and RM 8851, respectively, determined from

Table 13
Information values obtained by particle sizing methods for RM 8850

Cumulative volume (%)	Laser light scattering mean diameter (μm)[a]	Electric sensing zone mean diameter (μm)[a]	Laser light extinction mean diameter (μm)[b]	X-ray sedimentation mean diameter (μm)
10	0.566 ± 0.004	1.12 ± 0.02	1.37 ± 0.04	0.77
25	1.012 ± 0.006	1.44 ± 0.03	2.50 ± 0.06	1.13
50	1.908 ± 0.009	1.99 ± 0.02	4.42 ± 0.08	1.66
75	3.455 ± 0.017	3.19 ± 0.03	7.00 ± 0.10	2.70
90	5.587 ± 0.036	5.43 ± 0.11	9.08 ± 0.06	4.56

[a] Uncertainty values represent the standard deviation of the mean.
[b] Uncertainty values are expanded uncertainties with coverage factor $k = 2$ (95% confidence).

Table 14
Information values obtained by particle sizing methods for RM 8851

Cumulative volume (%)	Laser light scattering mean diameter (μm)[a]	Electric sensing zone mean diameter (μm)[a]	Laser light extinction mean diameter (μm)[b]	X-ray sedimentation mean diameter (μm)
10	1.285 ± 0.003	1.93 ± 0.01	1.75 ± 0.04	1.48
25	1.691 ± 0.004	2.32 ± 0.01	2.69 ± 0.06	1.87
50	2.339 ± 0.006	2.81 ± 0.02	3.86 ± 0.07	2.37
75	3.276 ± 0.012	3.44 ± 0.03	5.30 ± 0.08	3.10
90	4.541 ± 0.021	4.85 ± 0.09	8.97 ± 0.06	4.45

[a] Uncertainty values represent the standard deviation of the mean.
[b] Uncertainty values are expanded uncertainties with coverage factor $k = 2$ (95% confidence).

Table 15
Information values obtained by particle sizing methods for RM 8852

Cumulative volume (%)	Laser light scattering mean diameter (μm)[a]	X-ray sedimentation mean diameter (μm)[b]
10	0.268 ± 0.002	0.21
25	0.350 ± 0.001	0.30
50	0.484 ± 0.001	0.45
75	0.712 ± 0.005	0.74
90	1.698 ± 0.043	1.41

[a] Uncertainty values represent the standard deviation of the mean.
[b] Values for X-ray sedimentation are included for particle diameters less than 0.5 μm but the values are less reliable than those from larger particles due to Brownian motion.

the chemical homogeneity study done by XRF. These samples were loaded into sample holders and sealed under dry He prior to the neutron diffraction work so that humidity variation is not expected to be a factor.

3.3. Particle size analyses

Refractive index measurements obtained for Mie modeling of particle size for the light scattering method are given in Table 12. Comparisons of the cumulative volume percent less than a given diameter obtained by four particle sizing methods for RM 8850 and RM 8851 are given in Tables 13 and 14. Comparison of the cumulative volume percent less than a given diameter obtained by two particle sizing methods for RM 8852 is given in Table 15. Plots of the distributions obtained from the laser light scattering and the electric sensing zone methods are given in Figs. 5 and 6. Images of the samples obtained by dark field STEM are given in Fig. 7. RM 8851 has particles with the most euhedral appearance.

4. Discussion

4.1. Mass variation with RH variation

Yang and Navrotsky [32] discuss variation in sample mass with variation in RH for a series of cationic exchanged zeolite Y structures. They reported that LiY, NaY, KY, RbY, CsY and CaY may gain up to 2% in mass as RH is varied from low humidity (15% ± 3%) to high
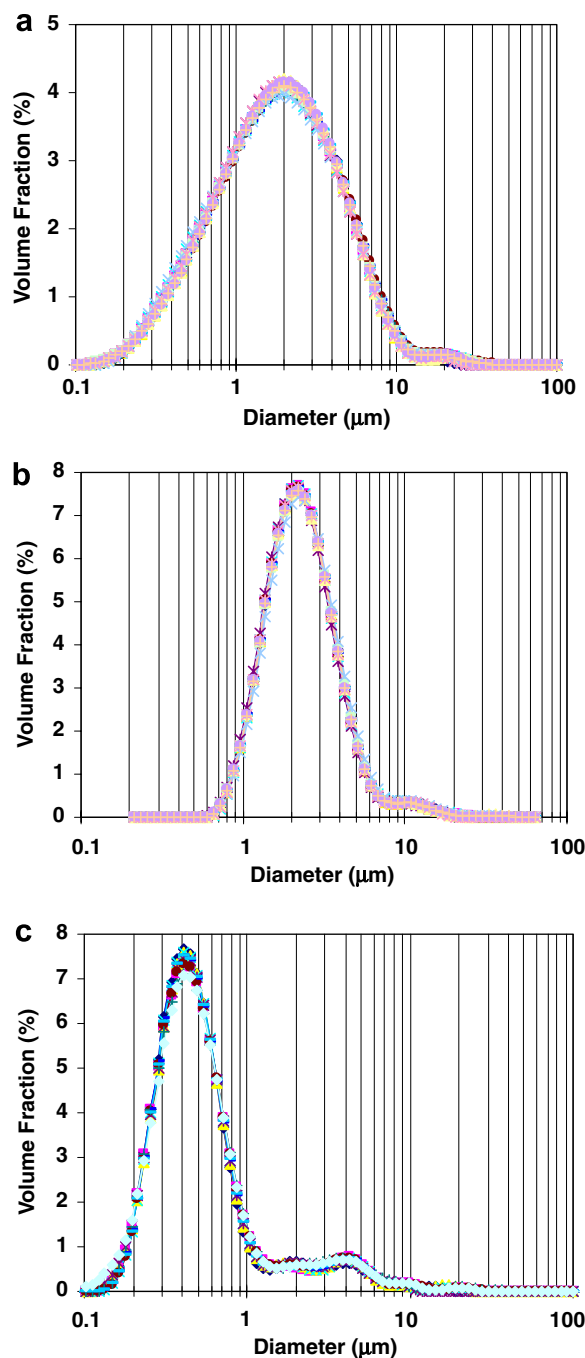

Fig. 5. Distribution of differential volume fraction (%) vs. particle diameter as measured by the laser light scattering method for (a) RM 8850, (b) RM 8851, and (c) RM 8852. Each curve represents the analysis for a different bottle of the eight bottles analyzed.
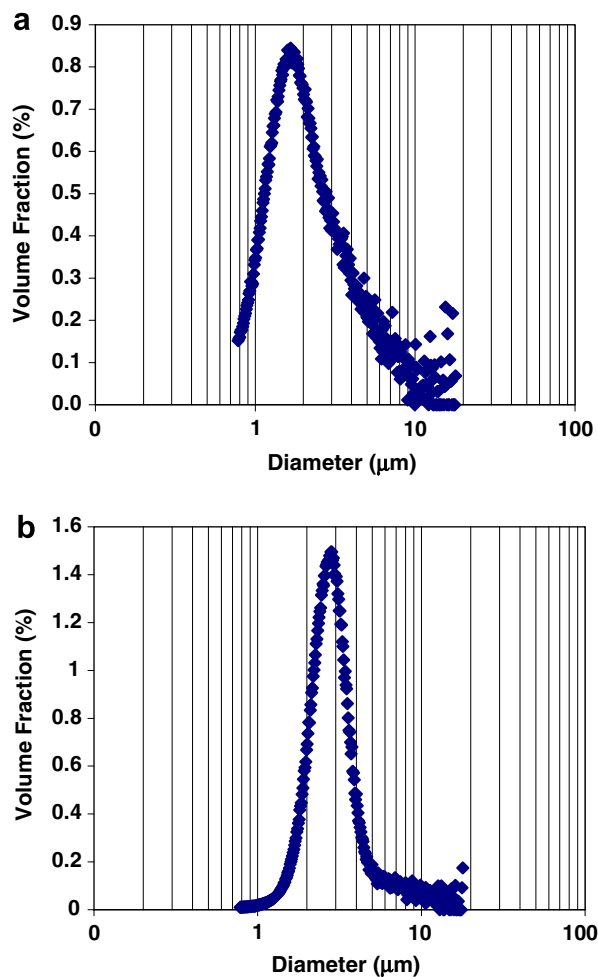
Fig. 6. Distribution of differential volume fraction (%) vs. particle diameter as measured by the electric sensing zone method for (a) 8850 and (b) 8851.

RM 8851. For RM 8851, the minor sodalite component (presumed $Na_8Al_6Si_6O_{24}Cl_2$) when normalized to 384 O has a formula of $Na_{128}Al_{96}Si_{96}O_{384}Cl_{32}$. The amount of

Fig. 7. Dark field STEM images of (a) RM 8850, (b) RM 8851, and (c) RM 8852.

humidity (90% ± 3%) at room temperature. HY and LaY show greater than 5% change in mass under similar conditions. This variation in mass is attributed to adsorption of surface water (physical adsorption). The mass gain determined in this work for zeolite Y (0.5%) is comparable given the smaller variation in humidity (33% ± 2% RH to 54% ± 2% RH).

4.2. Formulas and element ratios

Formulas for the reference materials are given in Table 16. The formulas are derived from the mass fraction percents given for the major components in Table 3. For RM 8852, NH_4^+ is presumed to provide charge balance for the Al content.

These formulas are derived from the bulk content of the materials and therefore may reflect contributions from impurities. No crystalline impurities in the RM 8852 material were detected by diffraction work, however, a minor amount of an unknown impurity was detected in RM 8850 and a minor amount of sodalite was detected in

Table 16
Formulas for RM 8850, RM 8851 and RM 8852

Material	Zeolite	Formula[a,b]
RM 8850	Zeolite Y	$Na_{54.0}Al_{54.1}Si_{137.9}O_{384} \cdot 245.1H_2O$
RM 8851	Zeolite A	$Na_{97.3}Al_{96.2}Si_{95.5}O_{384} \cdot 209.4H_2O$
RM 8852	Ammonium ZSM-5	$(NH_4)_{3.27}Al_{3.27}Si_{92.73}O_{192} \cdot 26.7H_2O$

[a] The formula for zeolite Y likely includes a contribution from a unidentified impurity phase. The formula for zeolite A includes a minor sodalite component. See text for discussion.

[b] The uncertainties for the elemental and water content in the formula for zeolite Y are: Na ± 0.7, Al ± 0.7, Si ± 1.0, H_2O ± 0.9; for zeolite A are: Na ± 0.5, Al ± 0.5, Si ± 0.6, H_2O ± 0.8; for ZSM-5 are: Al ± 0.04, Si ± 0.8, combined H_2O and NH_3 ± 0.3. The uncertainties are propagated from the uncertainties in mass fraction percent given in Table 3. Trace elements have not been included in the formulas. It is assumed that only water is lost during ignition of zeolite Y and zeolite A and that only water and ammonia are lost during ignition of ammonium ZSM-5.

Al and Si in sodalite is equivalent to that in zeolite A, but the amount of Na is greater by 33%. Therefore, a sodalite impurity increases the amount of Na relative to Al and Si that would be derived from an analysis of a pure zeolite A sample. Indeed, the formula in Table 16 shows approximately 1% more Na than Al. Assuming this difference is solely attributable to sodalite, this would translate to an approximate 3% sodalite content. This is comparable to the upper limit of 2% found by modeling detection limits in the neutron diffraction work given the uncertainty in the compositional data. The presence of sodalite, which is anhydrous, suppresses the water content of the bulk material. The zeolite A component of RM 8851 would therefore have higher water content than shown in Table 16.

The Na/Al for RM 8851 reported in Table 4 is 1.0120 ± 0.0074. The fact that the value is slightly >1 might be explained again in part by the presence of sodalite as a component of the material. Sodalite has an elevated Na/Al ratio of 1.33. Assuming a 2% sodalite content in a zeolite A

material, the combined Na/Al ratio expected from elemental analysis would be 1.0066.

Two Si/Al ratios are reported for both RM 8850 and RM 8851 in this work. In Table 4, the ratios are derived from the elemental concentrations and in Table 6, the ratios are determined from ^{29}Si MAS NMR analyses. The ^{29}Si MAS NMR analyses of Si/Al reflect the composition of the zeolitic framework only [31]. The bulk Si/Al ratio as determined from elemental analyses reflects the ratio of Si and Al present in the framework and outside the zeolite framework. If aluminum is present in the pores as a result of framework dealumination or if aluminate is present as inclusions from synthesis, the bulk Si/Al ratio will be lower than the ratio determined from ^{29}Si MAS NMR. Conversely, if excess Si is present as nonzeolite material such as amorphous components or due to lattice defects, the Si/Al ratio determined by bulk analyses will be higher than determined by ^{29}Si MAS NMR. Comparisons of Si/Al ratios determined by bulk methods and by ^{29}Si MAS NMR for nine zeolites of various compositions showed a percent deviation ranging from −38% to +300% [31]. Comparison of the Si/Al ratio determined by bulk, elemental analyses to ^{29}Si MAS NMR for RM 8850, show values of 2.548 ± 0.037 (Table 4) and 2.60 ± 0.06 (Table 6), respectively. The closeness in values likely is consistent with a zeolite sample without extra-framework Si or Al. For RM 8851, the Si/Al ratio of 0.9935 ± 0.0082 is within experimental uncertainty of the value = 1 estimated from the ^{29}Si MAS NMR spectra. This Si/Al ratio would not be affected by the sodalite inclusions, which have an ideal Si/Al ratio = 1.

4.3. Unit cell parameters

Considerable work has been done to relate the aluminum content of the hydrated zeolite Y structure to the unit
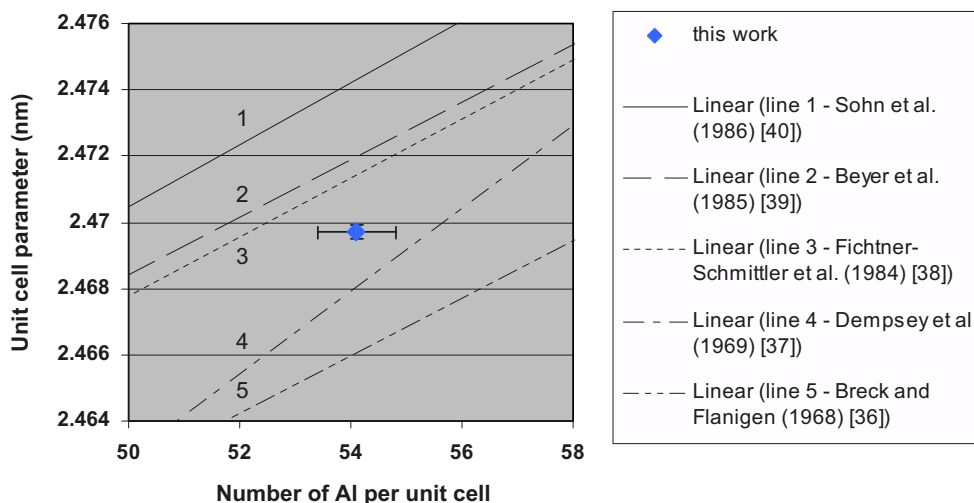

Fig. 8. Plot of the *a* unit cell parameter for hydrated zeolite Y against aluminum content per unit cell for values obtained from the literature and in this work. The correlation coefficients calculated or reported for data used to determine lines 1, 3 and 4 are 0.999, 0.984 and 0.996 (the data used to determine lines 2 and 5 were not reported and therefore correlation coefficients could not be calculated). The analytical error for the *a* unit cell parameters used to determine the linear relations was reported as ±0.0005 nm or less for lines 1, 3, 4, and 5.

cell size [36–40]. In general, a linear relationship is derived where unit cell parameter increases with increased framework aluminum content and such relationships are commonly used to estimate framework aluminum content [41–43]. A comparison of selected linear relationships obtained in the literature to the data obtained in this work for hydrated zeolite Y is shown in Fig. 8. The unit cell parameter value obtained in this work is higher than the projected value for Dempsey et al. [37] and Breck and Flanigen [36] and (lines 4 and 5) but lower than that for Sohn et al. [40], Beyer et al. [39] and Fitchtner-Schmittler et al. [38] (lines 1–3). The higher unit cell values for lines 1–3 may result from the use of samples in these studies in which Na^+ was partly or wholly exchanged with NH_4^+. Such ammonium exchange can lead to an increased lattice parameter [44]. The samples used for lines 4 and 5 were untreated Na-Y and should therefore be more comparable to the zeolite Y in this study. The reason for the higher unit cell parameter for zeolite Y in this study relative to lines 4 and 5 is not known. However, it is interesting to note that Dempsey et al. (1969) (line 4) collected their data from samples equilibrated at an RH of 75%. The unit cell parameter determined in the present work at $54\% \pm 2\%$ RH is slightly larger than the value determined from the Dempsey linear relationship. This is qualitatively consistent with the fact that the dehydrated zeolite Y unit cell is larger than the hydrated material [45].

A comparison of unit cell parameter values to selected literature values for dehydrated zeolite Y, for hydrated and dehydrated zeolite A and for hydrated ZSM-5 is shown in Table 17. The ambient RH was not given for the unit cell values reported in the literature for hydrated zeolite A and ZSM-5.

5. Summary

Three reference materials: RM 8850 (zeolite Y), RM 8851 (zeolite A) and RM 8852 (ammonium ZSM-5 zeolite) have been produced. The materials were reduced in sample size by spin riffling and were packaged in bottles in units of 35–40 g. The three materials have been characterized by a variety of chemical, diffraction and particle sizing methods. The materials have been assigned reference values for bulk and trace composition and for Si/Al and Na/Al ratios. Information values are given for enthalpies of formation, unit cell parameters and particle size distributions, refractive indices and variation of mass with variation in RH.

Table 17
Comparison of cell parameters in literature to those obtained in this work for zeolite Y (dehydrated), zeolite A (hydrated and dehydrated) and ZSM-5 (hydrated)

Material	Unit cell parameters (nm)[a]	Si/Al ratio	Reference
Zeolite Y			
Dehydrated	$a = 2.471$ (2)	2.37	Eulenberger et al. [46]
Dehydrated	$a = 2.47314$ (9)	2.58	Grey et al. [47]
Dehydrated	$a = 2.4791$ (3)	2.548 ± 0.037	This work
Zeolite A			
Hydrated	$a = 2.461$ (1)		Gramlich and Meier [48]
Hydrated	$a = 2.4588$		Pikus et al. [49]
Hydrated	$a = 2.4589$ (2)		This work
Dehydrated	$a = 2.4555$ (2)		Pluth and Smith [50]
Dehydrated	$a = 2.4560$ (6)		This work
ZSM-5			
Hydrated	$a = 2.0100$ (4) $b = 1.9959$ (4) $c = 1.3409$ (4)	25	Chao et al. [51]
Hydrated	$a = 2.0116$ (8) $b = 1.9931$ (14) $c = 1.3418$ (9)	28.34 ± 0.39	This work

[a] The numbers in parentheses are error estimates or uncertainties given in the cited reference. The cell parameters obtained by Pikus et al. (2004) for hydrated zeolite A are doubled from those reported.

References

[1] M.E. Davis, Nature 417 (2002) 813.
[2] T.F. Degnan, G.K. Chitnis, P.H. Schipper, Micropor. Mesopor. Mater. 35–36 (2000) 245.
[3] D.W. Breck, Zeolite Molecular Sieves, John Wiley & Sons, New York, 1974.
[4] G. Grubert, M. Stockenhuber, O.P. Tkachenko, M. Wark, Chem. Mater. 14 (2002) 2458.
[5] J. Caro, M. Noack, P. Kölsch, R. Schäfer, Micropor. Mesopor. Mater. 38 (2000) 3.
[6] Z. Lai, G. Bonilla, I. Diaz, J.G. Nery, K. Sujaoti, M.A. Amat, E. Kokkoli, O. Terasaki, R.W. Thompson, M. Tsapatsis, D.G. Vlachos, Science 300 (2003) 456.
[7] C.D. Johnson, F. Worrall, Micropor. Mesopor. Mater. 73 (2004) 191.
[8] C.A. Fyfe, D.H. Brouwer, Micropor. Mesopor. Mater. 39 (2000) 291.

[9] K. Ha, J.S. Park, K.S. Oh, Y.-S. Zhou, Y.S. Chun, Y.-J. Lee, K.B. Yoon, Micropor. Mesopor. Mater. 72 (2004) 91.

[10] E.N. Coker, J.C. Jansen, F. DiRenzo, F. Fajula, J.A. Martens, P.A. Jacobs, A. Sacco Jr., Micropor. Mesopor. Mater. 46 (2001) 223.

[11] K. Yamamoto, Y. Sakata, Y. Nohara, Y. Takahashi, T. Tatsumi, Science 300 (2003) 470.

[12] www.bam.de.

[13] W. May, R. Parris, C. Beck, J. Fassett, R. Greenberg, F. Guenther, G. Kramer, S. Wise, T. Gills, J. Colbert, R. Gettings, B. MacDonald, NIST Special Publication 260-136, US Government Printing Office, Washington, DC, 2000.

[14] Report of Investigation, Reference Material 8850, NIST, Gaithersburg, MD, USA.

[15] Report of Investigation, Reference Material 8851, NIST, Gaithersburg, MD, USA.

[16] Report of Investigation, Reference Material 8852, NIST, Gaithersburg, MD, USA.

[17] www.nist.gov/srm/.

[18] ASTM E 104-02, Standard Practice for Maintaining Constant Relative Humidity by Means of Aqueous Solutions, Annu. Book of Stand., vol. 11.03, West Conshohocken, PA.

[19] J.R. Sieber, Adv. X-ray Anal. 45 (2002) 493.

[20] R.R. Greenberg, R.F. Fleming, R. Zeisler, Environ. Int. 10 (1984) 129.

[21] A. Navrotsky, Phys. Chem. Miner. 2 (1977) 89.

[22] I. Kiseleva, A. Navrotsky, I.A. Belitsky, B.A. Fursenko, Am. Mineral. 81 (1996) 658.

[23] I. Kiseleva, A. Navrotsky, I.A. Belitsky, B.A. Fursenko, Am. Mineral. 81 (1996) 668.

[24] A. Le Bail, H. Duroy, J.L. Fourquet, Mater. Res. Bull. 23 (1988) 447.

[25] A.C. Larson, R.B. von Dreele, Los Alamos National Laboratory Report LAUR 86-748, 2004.

[26] www.ncnr.nist.gov.

[27] Guide to the Expression of Uncertainty in Measurement, International Organization for Standardization, Geneva, Switzerland, 1995.

[28] M.S. Levenson, D.L. Banks, K.R. Eberhardt, L.M. Gill, W.F. Guthrie, H.K. Liu, M.G. Vangel, J.H. Yen, N.F. Zhang, J. Res. Natl. Inst. Stand. Technol. 105 (2000) 571.

[29] B.N. Taylor, C.E. Kuyatt, NIST Technical Note 1297, U.S. Government Printing Office, Washington DC, 1994.

[30] H.H. Ku, J. Res. Natl. Bur. Stand. 70C (1966) 263.

[31] D.R. Corbin, B.F. Burgess Jr., A.J. Vega, R.D. Farlee, Anal. Chem. 59 (1987) 2722.

[32] S. Yang, A. Navrotsky, Micropor. Mesopor. Mater. 37 (2000) 175.

[33] S. Yang, A. Navrotsky, Micropor. Mesopor. Mater. 41 (2000) 345.

[34] P.M. Piccione, C. Laberty, S. Yang, M.A. Camblor, A. Navrotsky, M.E. Davis, J. Phys. Chem. B 104 (2000) 10001.

[35] D. Schwarzenbach, S.C. Abrahams, H.D. Flack, E. Prince, A.J.C. Wilson, Acta Crystallogr. A51 (1995) 565.

[36] D.W. Breck, E.M. Flanigen, Molecular Sieves, Society of Chemical Industry, London, 1968, pp. 47–61.

[37] E. Dempsey, G.H. Kühl, D.H. Olson, J. Phys. Chem. 73 (1969) 387.

[38] H. Fitchtner-Schmittler, U. Lohse, G. Engelhardt, V. Patzelová, Cryst. Res. Technol. 19 (1984) K1.

[39] H.K. Beyer, I.M. Belenykaja, F. Hange, M. Tielen, P.J. Grobet, P.A. Jacobs, J. Chem. Soc., Faraday Trans. I 81 (1985) 2889.

[40] J.R. Sohn, S.J. DeCanio, J.H. Lunsford, D.J. O'Donnell, Zeolites 6 (1986) 225.

[41] J.G. Nery, M.V. Giotto, Y.P. Mascarenhas, D. Cardoso, F.M.Z. Zotin, E.F. Sousa-Aguiar, Micropor. Mesopor. Mater. 41 (2000) 281.

[42] W. Lutz, C.H. Rüscher, D. Heidemann, Micropor. Mesopor. Mater. 55 (2002) 193.

[43] K. Sato, Y. Nishimura, N. Matsubayashi, M. Imamura, H. Shimada, Micropor. Mesopor. Mater. 59 (2003) 133.

[44] J.A. Kaduk, J. Faber, Rigaku J. 12 (1995) 14.

[45] J.A. Rubio, J. Soria, F.H. Cano, J. Colloid Interf. Sci. 73 (1980) 312.

[46] G.R. Eulenberger, D.P. Shoemaker, J.G. Keil, J. Phys. Chem. 71 (1967) 1812.

[47] C.P. Grey, F.I. Poshni, A.F. Gualtieri, P. Norby, J.C. Hanson, D.R. Corbin, J. Am. Chem. Soc. 119 (1997) 1981.

[48] V. Gramlich, W.M. Meier, Z. Kristallogr. 133 (1971) 134.

[49] S. Pikus, E. Olszewska, M. Majdan, L. Pajak, Powder Diffr. 19 (2004) 172.

[50] J.J. Pluth, J.V. Smith, J. Am. Chem. Soc. 102 (1980) 4704.

[51] K.-J. Chao, J.-C. Lin, Y. Wang, G.H. Lee, Zeolites 6 (1986) 35.